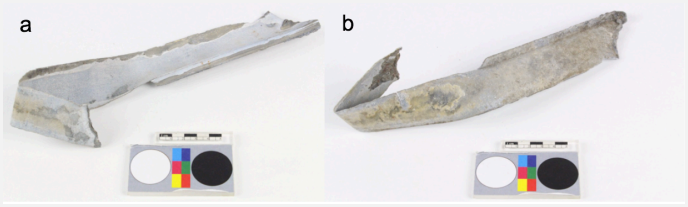
ROOF GUTTER ELEMENT – ZN ALLOY – MODERN TIMES – FRANCE

Artefact name	Roof gutter element
Authors	Christian. Degrigny (HE-Arc CR, Neuchâtel, Neuchâtel, Switzerland) & Mathea. Hovind (University of Oslo, Department of archaeology, conservation and history (IAKH-UiO), Oslo, Oslo, Norway)
Url	/artefacts/403/

The object



Credit UiO-IAKH, M.Hovind.

Fig. 1: Zn flashing, surface “a” and “b”, to the left and right, respectively,

Description and visual observation

Description of the artefact	A piece of zinc flashing with remains of lead solder (Fig. 1). Its surfaces are covered by a white, strongly adherent oxide layer. Surface “b” is slightly darker in colour than surface “a” due to the presence of soil particles. Dimensions: L = 265mm; W = 47mm; T = 1mm; WT = 93g.
Type of artefact	Architectural element
Origin	Château de Germolles, Mellecey, Bourgogne, France
Recovering date	Unknown
Chronology category	Modern Times
chronology tpq	1900 A.D.
chronology taq	2000 A.D.
Chronology comment	1900 AD/20th century
Burial conditions / environment	Outdoor atmosphere
Artefact location	Haute Ecole Arc Conservation-Restauration
Owner	Château de Germolles, Mellecey, Bourgogne
Inv. number	None
Recorded conservation data	Not conserved

This work is licensed under CC BY-NC-ND 4.0

Complementary information

Nothing to report.

Study area(s)



Credit UiO-IAKH, M.Hovind.

Fig. 2: Location of sampling area (a cross-section through the metal marked by the stippled line) and of powder samples (red circles),

Binocular observation and representation of the corrosion structure

The schematic representation below (Fig. 3) gives an overview of the corrosion layers encountered on the object from a first visual macroscopic observation.



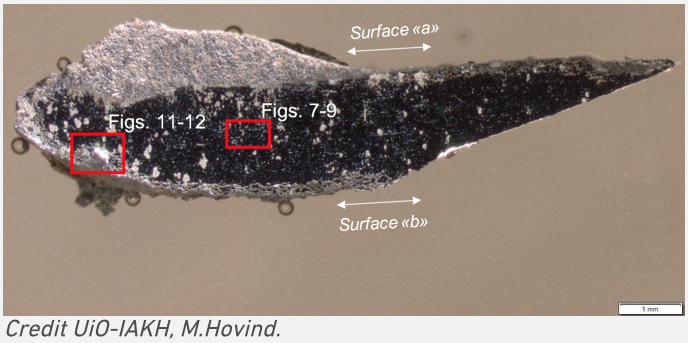
Captions	Description
D1	Remains of lead solder.
S1	Light brown and porous soil. Located only on surface "b".
CP1	Light grey to white, thin and adherent layer. Located on both surfaces.
M1	Intact metal. Submetallic and light grey in colour.

Credit UiO-IAKH, M.Hovind.

Fig. 3: Schematic presentation of the artefact (a cross-section of the metal) based on visual macroscopic observation. CP = corrosion product, D = deposit, M = metal, S = soil,

MiCorr stratigraphy(ies) – Bi

Sample(s)



Credit UiO-IAKH, M.Hovind.

Fig. 4: Micrograph of the sample showing the locations of Figs. 7-9 and 11-12. The uppermost area (in white) is remains of solder, while the zinc metal appears dark grey to black (the white patches are due to secondary oxidation of the sample),

Description of sample

A cross-section (Fig. 4) was cut out where the metal is at an angle of approximately 90° to the flat surface. Its upper edge corresponds to surface "a" and contains remains of solder, while the lower edge corresponds to surface "b".

This work is licensed under CC BY-NC-ND 4.0

Alloy	Zn Alloy
Technology	None
Lab number of sample	ZG2018 (zinc gutter sampled in 2018)
Sample location	Haute Ecole Arc Conservation-Restauration
Responsible institution	Haute Ecole Arc Conservation-Restauration
Date and aim of sampling	March 2018, metallography and chemical analyses

Complementary information

The fact that the fragment was considered a test material enabled extensive sampling that would not otherwise be possible.

Analyses and results

Metallography

Microscope: Leica DMi8 (a metallographic, inverted, reflected light microscope) with magnification up to 500X. Camera: Olympus SC50 connected to the software "Olympus Stream", version 1.9.4. Illumination modes: bright field and cross-polarized light.

SEM-EDS

Instrument: Jeol 6400; voltage: 20 kV; working distance: 18 and 24mm; sample preparation: palladium depot.

XRD

Diffractometer system: XPERT-3; Sample stage: Reflection-Transmission Spinner PW3064/60; Anode material: Cu.

Non invasive analysis

Metal

The flashing is composed of Zn with P and Pb (Fig. 6). The latter is probably originating from the solder that was applied to adjoin several metal sheets for the flashings.

The metal appears white to light grey under bright field (Fig. 7). Under polarized light however (Fig. 8), the microstructure of the metal is visible as small polygonal grains appearing in various shades of brown, a coloured effect due to the anisotropic properties of the metal (Scott 1991: 49). In the SEM-image, white elongated inclusions are visible (Fig. 9) consisting mainly of Zn and Pb with some O (Fig. 10).

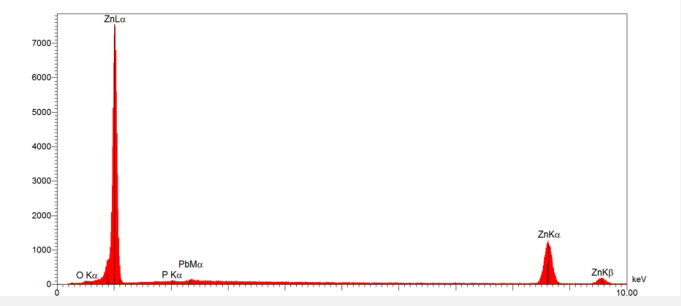
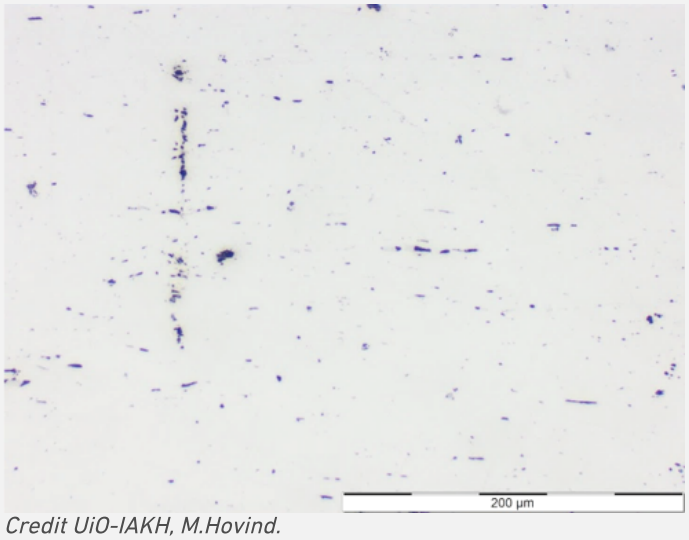


Fig. 6: Chemical composition of the metal. Method of analysis: SEM-EDS. Lab. of Electronic Microscopy and Microanalysis, Néode, HEI Arc,

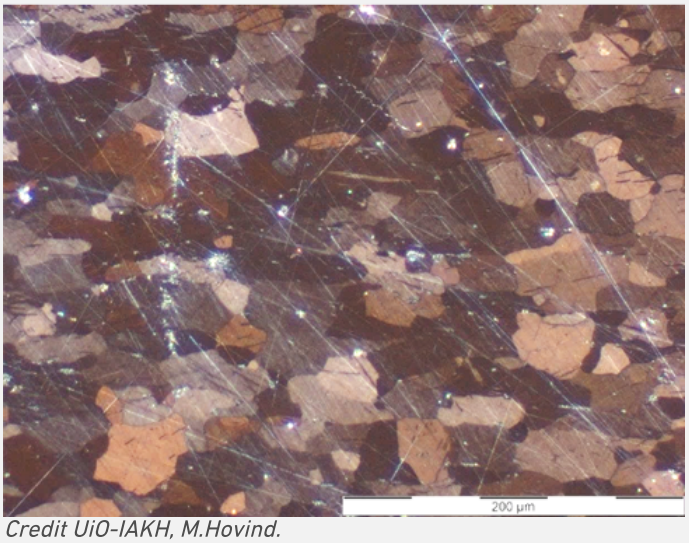
This work is licensed under CC BY-NC-ND 4.0

Credit HEI Arc, C.Csefalvay.



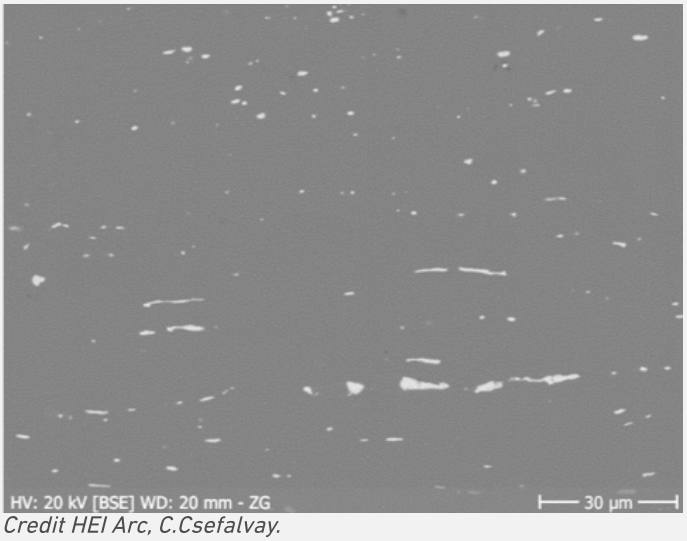
Credit UiO-IAKH, M.Hovind.

Fig. 7: Micrograph of the metal sample from Fig. 4 (detail). Unetched, bright field,



Credit UiO-IAKH, M.Hovind.

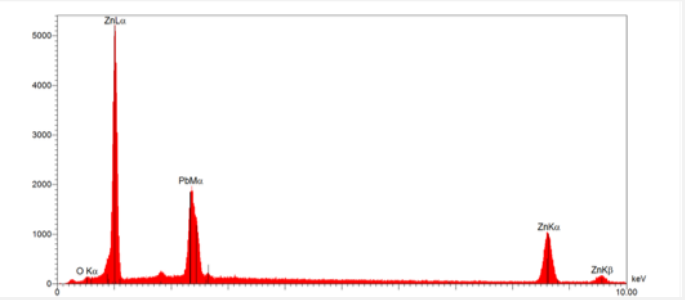
Fig. 8: Micrograph similar to Fig. 7, but under polarized light.The microstructure of the metal shows the presence of small and polygonal grains in shape,



Credit HEI Arc, C.Csefalvay.

Fig. 9: SEM-image (BSE-mode) of the metal sample from Fig. 4 (detail) showing the white elongated inclusions,

This work is licensed under CC BY-NC-ND 4.0



Credit HEI Arc, C.Csefalvay.

Fig. 10: SEM-EDS spectrum showing the composition of the elongated inclusions from Fig. 9. Method of analysis: SEM-EDS. Lab. of Electronic Microscopy and Microanalysis, Néode, HEI Arc,

Microstructure	None
First metal element	Zn
Other metal elements	P, Pb

Complementary information

Nothing to report.

Corrosion layers

The metal is suffering from intergranular corrosion visible as a white corrosion product (CP1) located within crevices and along the grain boundaries (Figs. 11 and 12). Both the corrosion product (CP1) and the corroded metal (CM1) appear dark grey in bright field (Fig. 11) and white under polarized light (Fig. 12). They both consist of Zn and O (Table 1). The external corrosion product (CP1) contains some S (and not Pb as suggested by Table 1 and Fig. 14) which is probably due to atmospheric pollution. The structural composition of the corrosion product was determined by crystallographic analysis (XRD) to consist of a mixture of zincite (ZnO) and pure zinc (Zn) (Table 2, Fig 13). Mapping of the corroded area by SEM-EDS displays a similar composition but shows additionally the presence of Cl in some of the cracks (Fig. 14).

Elements mass%*	C	O	Zn	Pb	S	Al	Si	Fe	Cu	Sn
CP1, white corrosion product	7	33	51	3	5	-	0.3	0.1	0.1	0.4
CM1, intergranular corrosion	6	22	68	3	0.1	0.1	0.1	0.1	0.1	0.5

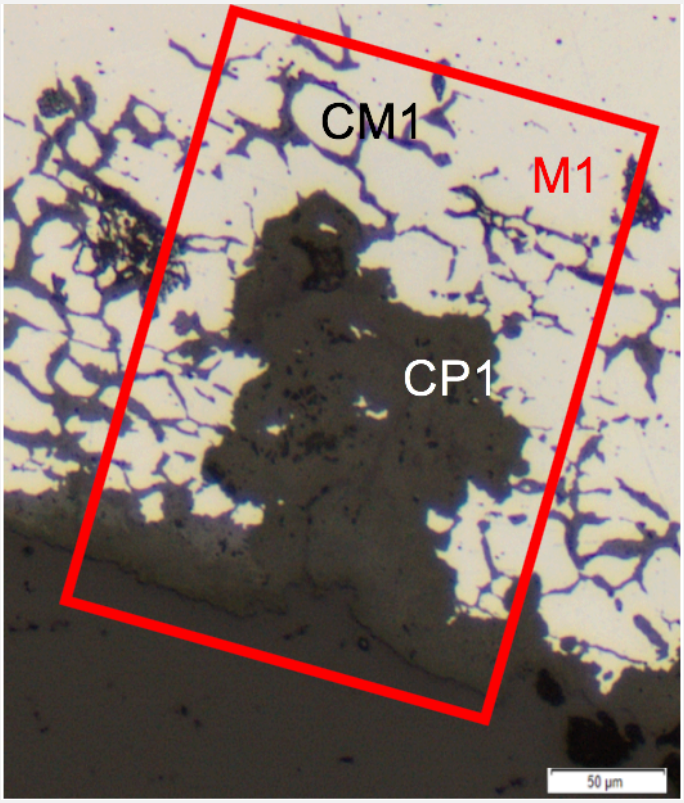
Table 1: Chemical composition of the corrosion layers from Fig. 11. Method of analysis: SEM-EDS. Lab. of Electronic Microscopy and Microanalysis, Néode, HEI Arc, credit MiCorr_HEI Arc, C.Csefalvay. *The sum is the calculated average of three analyses of the same feature, but in different areas.

Stratum	Components*
CP1	Zincite (ZnO), Zinc (Zn)

Table 2: Summary of the results from the crystallographic analysis of the white corrosion product (CP1). A representative spectrum is given in Fig. 13. Method of analysis: XRD. Center of X-ray Analytics, Empa-Swiss Federal Laboratories for

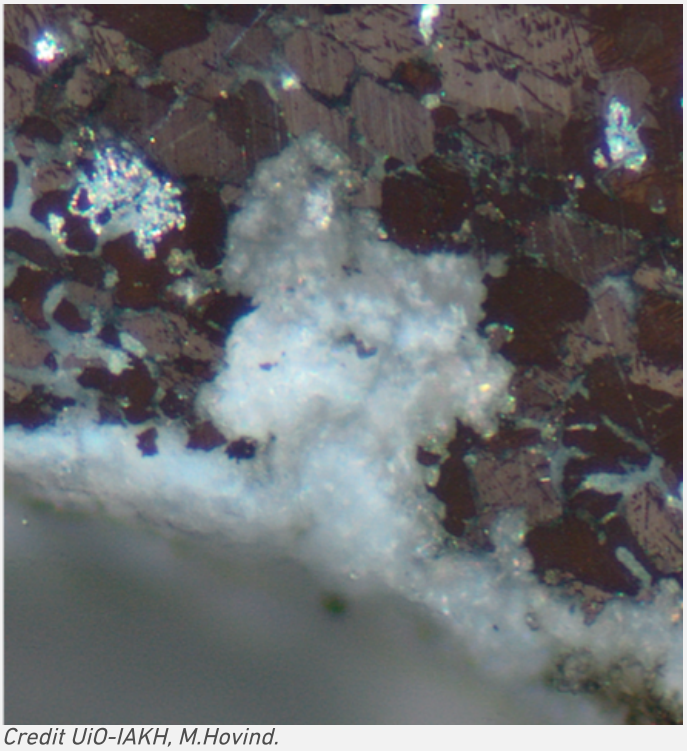
This work is licensed under CC BY-NC-ND 4.0

Materials Science and Technology (Dübendorf), credit MiCorr_Empa, Z.Balogh-Michels. *The results are based on the analysis of two powder samples from different areas (see Fig. 2 for sample locations).



Credit UiO-IAKH, M.Hovind.

Fig. 11: Micrograph of the metal sample from Fig. 4 (detail). Unetched, bright field. The corrosion product (CP1) is located at the surface of the metal and in its crevices. Intergranular corrosion (CM1) is visible as thin grey lines in between the metal grains (M1). The area selected for elementary mapping (Fig. 14) is marked by a red square



Credit UiO-IAKH, M.Hovind.

Fig. 12: Micrograph similar to Fig. 11 but under polarized light, the corrosion product (CP1) and the corroded metal (CM1) appear white,

This work is licensed under CC BY-NC-ND 4.0

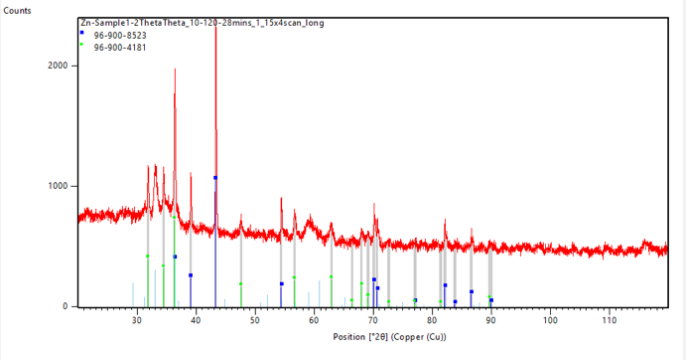


Fig. 13: XRD-spectrum for the analysis of powder sample 1. Ref. 96-900-8523 (in blue) corresponds to pure zinc and 96-900-4181 (in green) to zincite (ZnO),

Credit Empa, Z.Balogh-Michels.

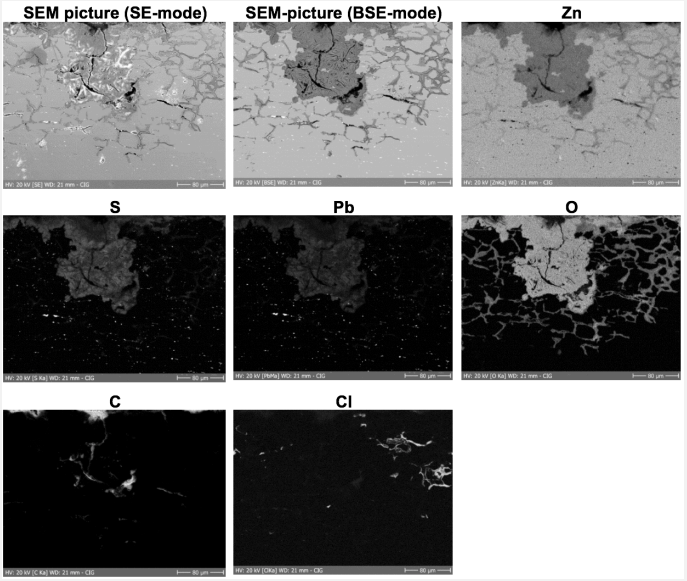


Fig. 14: SEM image and elemental chemical distribution of a selected area of Fig. 11 (rotated almost 180° and reversed). Method of analysis: SEM-EDS. Lab. of Electronic Microscopy and Microanalysis, Néode, HEI Arc,

Credit HEI Arc, C.Csefalvay.

Corrosion form	Crevice
Corrosion type	None

Complementary information

Nothing to report.

MiCorr stratigraphy(ies) – CS

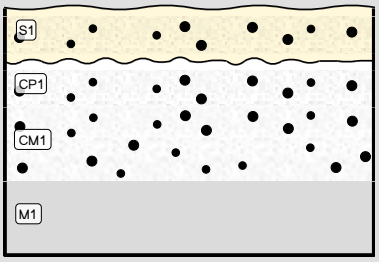
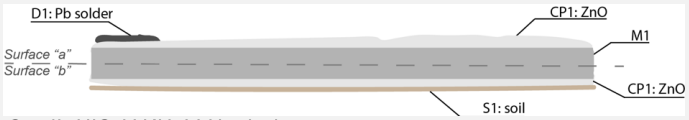


Fig. 5: MiCorr stratigraphy corresponding to the corrosion layers on surface “b” (Figs. 2 and 3). To be compared with Figs. 11 and 12, Credit UiO-IAKH, M.Hovind.

Synthesis of the binocular / cross-section examination of the corrosion structure

Nothing to report.

This work is licensed under CC BY-NC-ND 4.0



Credit UiO-IAKH, M.Hovind.

Fig. 15: Corrected stratigraphic representation with results from analyses by SEM-EDS, XRD and visual microscopic observation. CP = corrosion product, D = deposit, M = metal, S = soil,

Conclusion

The flashing consists of Zn with some Pb from the lead solder. It is covered by a strongly adherent layer of zincite (a zinc oxide), indicative of exposure to an unpolluted environment. Still, the metal exhibits intergranular corrosion, a deterioration phenomenon indicative of aggressive conditions. This can possibly be explained by the different locations of the samples. The cross-section studied is likely to correspond to the surface that was exposed to the atmosphere (surface "b"), while the powder samples were from the rear, unexposed surface (surface "a"). Exposure to moisture and low pH in the form of acidic rain are environmental parameters that would encourage intergranular corrosion. Furthermore, the presence of Cl inside the cracks could be due to pollution and its rather concealed location implies that it would be retained inside the metal and not washed away by rain (Selwyn 2004:153-154).

References

References sample:

1. Scott, D. A. (1991). Metallography and microstructure of ancient and historic metals. Marina del Rey, Calif.: Getty Conservation Institute in association with Archetype Books.

2. Selwyn, L. (2004). Metals and corrosion: A handbook for the conservation professional. Ottawa: Canadian Conservation Institute.

This work is licensed under CC BY-NC-ND 4.0